HHS Public Access

Author manuscript

*Cell Rep*. Author manuscript; available in PMC 2019 November 25.

Published in final edited form as:

*Cell Rep*. 2019 October 22; 29(4): 791–799.e3. doi:10.1016/j.celrep.2019.09.045.

# A Microglia Sublineage Protects from Sex-Linked Anxiety Symptoms and Obsessive Compulsion

**Dimitri Tränkner**[1,2,4,*], **Anne Boulet**[2], **Erik Peden**[2,3], **Richard Focht**[2], **Donn Van Deren**[2], **Mario Capecchi**[2,*]

[1]School of Biological Sciences, University of Utah, Salt Lake City, UT 84112, USA

[2]Department of Human Genetics, School of Medicine, University of Utah, Salt Lake City, UT 84112, USA

[3]Present address: Ivy Tech Community College—Central Indiana, School of Arts, Sciences, and Education, Science Department, Indianapolis, IN 46208, USA

[4]Lead Contact

## SUMMARY

Aberrant microglia activity is associated with many neurological and psychiatric disorders, yet our knowledge about the pathological mechanisms is incomplete. Here, we describe a genetically defined microglia sublineage in mice which has the ability to suppress obsessive compulsion and anxiety symptoms. These microglia derive from precursors expressing the transcription factor Hoxb8. Selective ablation of Hoxb8-lineage microglia or the *Hoxb8* gene revealed that dysfunction in this cell type causes severe over-grooming and anxiety-like behavior and stress responses. Moreover, we show that the severity of the pathology is set by female sex hormones. Together, our findings reveal that different microglia lineages have distinct functions. In addition, our data suggest a mechanistic link between biological sex and genetics, two major risk factors for developing anxiety and related disorders in humans.

## Graphical Abstract

*Correspondence: dimitri.trankner@gmail.com (D.T.), capecchi@genetics.utah.edu (M.C.).

AUTHOR CONTRIBUTIONS

D.T. and M.C. designed the experiments. D.T., E.P., A.B., R.F., and D.V.D. conducted the experiments. D.T. wrote the paper.

SUPPLEMENTAL INFORMATION

Supplemental Information can be found online at https://doi.org/10.1016/j.celrep.2019.09.045.

DECLARATION OF INTERESTS

The authors declare no competing interests.

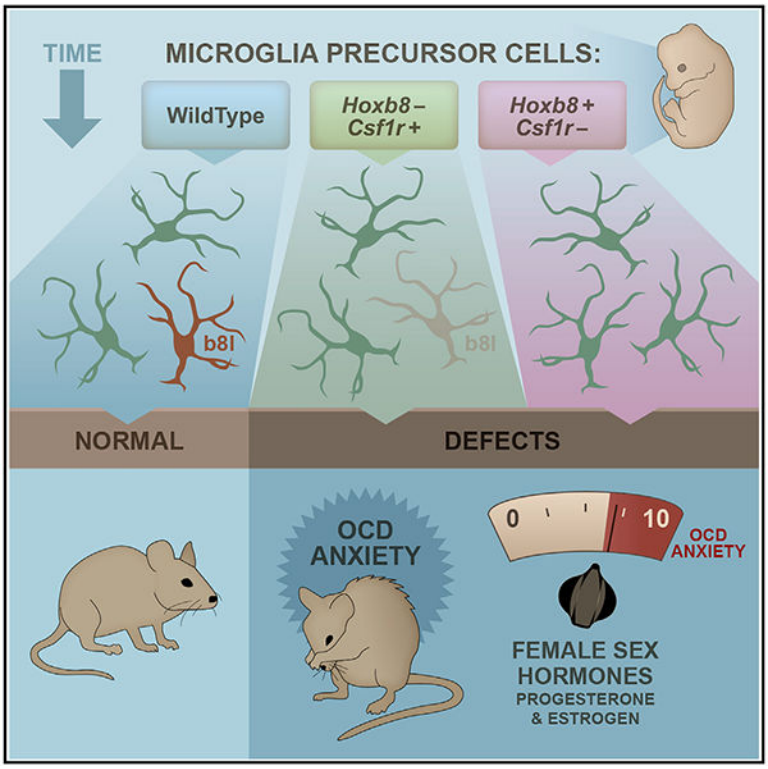


## In Brief

Tränkner et al. show that a microglia lineage uniquely suppresses OCD and anxiety in mice. The pathology caused by malfunction of this lineage is set by female sex hormones. The findings suggest a mechanistic link between biological sex and genetics, two major risk factors for anxiety related disorders in humans.

## INTRODUCTION

Microglia are the immune cells of the brain. A main function of microglia is to survey the local microenvironment and respond to injury by the release of pro-inflammatory molecules and phagocytic clearance of apoptotic cells (for review, see Lucin and Wyss-Coray, 2009). Microglia secretion and phagocytosis also control neuron and synapse density and synaptic plasticity in the healthy brain (Li and Barres, 2018; Schafer et al., 2012). Conversely, aberrant microglia activity can be pathogenic and is associated with symptoms in neurological disorders, including Alzheimer's and Parkinson's disease (Tejera and Heneka, 2016; Joe et al., 2018), and may cause depression or anxiety disorders under chronic stress (Stein et al., 2017; Ramirez et al., 2017; Li et al., 2014; Wang et al., 2018; McKim et al., 2018).

Microglia have been thought of as a homogeneous cell population with a common origin (Ginhoux and Guilliams, 2016). Single-cell RNA sequencing of microglia has revealed different cell signatures, but this has been interpreted to reflect distinct physiological states rather than different microglia subtypes (Hammond et al., 2019; for review, see Li and

Barres, 2018; Brioschi et al., 2019). However, we recently demonstrated that there are at least two different lineages of microglia, which may be programmed outside the brain for independent functions (De et al., 2018). Specifically, we found that a subset of microglia precursors express the transcription factor Hoxb8 during embryogenesis and undergo non-canonical and protracted expansion in the aorta-gonad-mesonephros (AGM) and fetal liver. Hoxb8-lineage microglia contribute approximately one-third of all microglia in the adult mouse brain (De et al., 2018). Interestingly, *Hoxb8* loss of function causes over-grooming (Chen et al., 2010), yet the exact cell type causing this pathology remains to be determined. Here, we report surprising aspects of the *Hoxb8* knockout (KO) pathology with high translational relevance and demonstrate that it is produced by loss of Hoxb8-lineage microglia function.

## RESULTS

### Hoxb8 Deletion Causes Sex-Linked Over-Grooming and Anxiety-like Behavior

Dysfunction of the homeobox transcription factor Hoxb8 in mice has previously been reported to cause severe coat loss due to over-grooming (Chen et al., 2010). Interestingly, close inspection of a large number of *Hoxb8* KO mice revealed that females consistently show more extreme coat loss and spend more time grooming than males (Figures 1A–1C). Motivated by these sex differences in *Hoxb8* KO mice, we further explored the pathology in females versus males. Over-grooming in mice shares characteristics with symptoms of obsessive compulsive disorder (OCD) in humans and is frequently used to model symptoms of this condition (Korff and Harvey, 2006; Chen et al., 2010). OCD is closely related to anxiety disorders, both are frequently comorbid (American Psychiatric Association, 2013), and OCD is often treated with anxiolytics (Bandelow, 2008). Given this tight relationship between OCD and anxiety in humans, we wondered whether *Hoxb8* KO mice show anxiety-like behavior and if it is sex-linked, too. We first measured anxiety-like behavior in an elevated plus maze. During the test, mice can choose between platform arms that are either open or enclosed by walls. Active avoidance of the open arms is interpreted as a sign of increased anxiety (Walf and Frye, 2007). We found that *Hoxb8* KO females consistently avoid the open arms and, consequently, spend more time on the closed arms than controls (Figure 1D) (Nagarajan et al., 2018). Intriguingly, we did not observe anxiety-like place avoidance in *Hoxb8* KO males. In conclusion, *Hoxb8* KO females, but not males, show anxiety-like behavior in addition to over-grooming.

### Hoxb8 Dysfunction Produces Marked Stress-Responses in Females

We further investigated the anxiety-like state in *Hoxb8* KO mice. Physiological stress responses are regulated by the hypothalamus, a brain region also recognized for its role in anxiety (Jimenez et al., 2018; Patriquin and Mathew, 2017). We hypothesized that physiological stress responses controlled by the hypothalamus, including release of cortisol (Pineda and Dooley, 2003) and fight-or-flight reflexes (Gellhorn, 1957), would be altered in mice in an anxiety-like state. We first confirmed this hypothesis with wild-type mice after treatment with the anxiogenic peptide urocortin II (Anthony et al., 2014; Henry et al., 2006). Cortisol levels and pupil fight-or-flight responses are significantly higher in urocortin II-treated than vehicle-treated mice of both sexes (Figure S1). We then tested *Hoxb8* KO mice,

and found that females show increased cortisol levels and pupil fight-or-flight responses compared to controls, similar to urocortin-treated mice (Figures 1E and 1F). *Hoxb8* KO males, however, lack altered stress-responses. This finding further distinguishes the *Hoxb8* KO pathology in females versus males and establishes that anxiety symptoms are also sex-linked in this mouse model.

## A Key Role of Female Sex Hormones in the *Hoxb8* KO Pathology

*Hoxb8* KO mice start showing coat loss at roughly 3 weeks of age and it becomes more severe in females at 6–8 weeks of age, which coincides with the onset of sexual maturity (Figure 2A). This suggests a role of sex hormones in the over-grooming pathology. We tested if female sex hormones exacerbate over-grooming by interfering with the synthesis of relevant steroids using two approaches. First, we treated *Hoxb8* KO females pharmacologically with trilostane. Trilostane blocks 3β-hydroxysteroid dehydrogenase, a key enzyme essential for the synthesis of most steroid hormones, including progesterone and 17β-estradiol (Potts et al., 1978). Second, we lowered female sex hormones, including progesterone and 17β-estradiol levels, by removing ovaries (Figures 2B and 2C). Daily pharmacological treatments were started and ovariectomies performed on 4-week-old mice, tests were performed 2 months later. Both trilostane treatment and ovariectomy limit coat loss to levels similar to those observed in age-matched *Hoxb8* KO males (Figures 2D and 2E). Consistent with reduced coat loss, trilostane-treated and ovariectomized females also spend less time grooming (Figure 2F). Most intriguingly, both treatments attenuate anxiety-like behavior (Figure 2G) and abnormal stress responses (Figure 2H, I). These effects are specific to the *Hoxb8* KO pathology as we did not observe changes in place preference or stress responses in ovariectomized wild-type mice (Figure S2). Finally, we directly tested if female sex hormones are sufficient to induce the severe, female *Hoxb8* KO pathology by injecting *Hoxb8* KO males with progesterone, 17β-estradiol, or both combined for 4 weeks. We then analyzed the mice for over-grooming using the coat-loss assay, anxiety-like behavior using the place-avoidance assay, and anxiety-like stress responses using the pupil dilation test. Although the pupil stress response did not increase to statistically significant levels after hormone treatment, the combination of progesterone and 17β-estradiol significantly worsens coat loss and produces anxiety-like place avoidance compared to vehicle alone (Figures 2J–2M). These effects are absent in wild-type males (Figure S2), substantiating a mechanistic link between Hoxb8 dysfunction and female sex hormones in producing the *Hoxb8* KO pathology.

## Testing the Role of Microglia in the Hoxb8 KO Pathology

The only cells derived from *Hoxb8*-expressing precursors in the brain and OCD-associated circuits belong to a subset of microglia. Moreover, experiments with cell-type-restricted *Hoxb8* ablation pointed to Tie2-lineage myeloid cells, including microglia, to be responsible for the pathology (Chen et al., 2010). It has, therefore, been hypothesized that Hoxb8-lineage microglia mediate the *Hoxb8* KO phenotype. We directly tested this hypothesis by selectively ablating Hoxb8-lineage microglia, hereafter abbreviated “b8l microglia,” in both *Hoxb8* KO and wild-type background. If the disease phenotype in *Hoxb8* KO mutants is mediated by gain of function in b8l microglia, then ablating this cell type should rescue the

pathology. Similarly, if the pathology is due to a loss of function in b8l microglia, then ablating this cell type should mimic the *Hoxb8* KO phenotype.

To selectively ablate b8l microglia, we disrupted the gene encoding the colony stimulating factor 1 receptor (*Csf1r*) exclusively in *Hoxb8*-expressing cells and their progeny. Signaling via Csf1r is essential for survival of all differentiated microglia and interference with Csf1r function is a widely used tool to ablate microglia (Li et al., 2006; Erblich et al., 2011; Elmore et al., 2014; Han et al., 2017; Nakayama et al., 2018; Krukowski et al., 2018). To achieve the cell ablation in wild-type *Hoxb8* mice, we generated transgenic mice that express Cre recombinase under the control of the *Hoxb8* promotor ($Hoxb8^{IRES\text{-}Cre}$) (Chen et al., 2010), a Cre-dependent conditional KO allele of *Csf1r* ($Csf1r^{flox}$) (Li et al., 2006), and the Cre-dependent reporter tdTomato ($Rosa26^{lsl\text{-}tdTomato}$) (Madisen et al., 2010) (Figure 3A). To achieve the cell ablation in *Hoxb8* KO mice, we generated $Hoxb8^{mut\text{-}IRES\text{-}Cre}$ with a disabled DNA binding domain. Mice homozygous for $Csf1r^{flox}$ lose Csf1r function in Hoxb8-expressing cells and should lack mature b8l microglia ($Csf1r^{-}$); mice with the same allele composite but one intact *Csf1r* allele preserve receptor function and serve as controls ($Csf1r^{+}$) (Figure 3B).

To test the efficiency of the ablation strategy, we counted tdTomato-expressing cells in brain tissue. In agreement with previous studies of mice that combine $Hoxb8^{IRES\text{-}Cre}$ with $Rosa26^{lsl\text{-}tdTomato}$, the only tdTomato-labeled cells in brain parenchyma are b8l microglia (Chen et al., 2010; De et al., 2018). Compared to controls, $Csf1r^{-}$ mice lose almost 90% of tdTomato labeled cells in both *Hoxb8* wild-type and KO background and independent of sex (Figures 3C and 3D). Interestingly, the total density of microglia in mice depleted of b8l microglia is similar to that of controls, suggesting that non-b8l microglia replace the missing b8l microglia population (Figures 3E and 3F). In contrast to systemic interference with Csf1r signaling (Dai et al., 2002; Erblich et al., 2011), loss of Csf1r function only in Hoxb8 cells did not produce gross anatomical or developmental abnormalities in mice, including the brain, nor did it affect non-parenchymal Hoxb8-lineage cells in the brain or blood-born monocytes (Figure 3S).

## Loss of b8l Microglia Function Is Sufficient to Produce the *Hoxb8* KO Pathology

If the *Hoxb8* KO disease phenotype is mediated by a gain of function in b8l microglia, then ablating this cell type should rescue the pathology. To test this possibility, we examined *Hoxb8* KO mice in which we ablated b8l microglia and found a coat-loss pattern, grooming time, elevated plus maze place preference, cortisol levels, and pupil fight-or-flight reflexes typical for *Hoxb8* KO mutants (Figure S4). Thus, depleting b8l microglia does not rescue the *Hoxb8* KO phenotype. The lack of rescue argues against a damaging gain of function in b8l microglia cells as the primary cause of the *Hoxb8* KO pathology. This still leaves the possibility that a loss of function in b8l microglia causes over-grooming and anxiety-like behavior. In fact, ablating b8l microglia in the *Hoxb8* wild-type background produces a pathology that closely phenocopies *Hoxb8* KO mutants. Readily apparent in these mice are coat loss on chest, forelimbs, and abdomen (Figures 4A–4C). Moreover, grooming time in *Hoxb8* wild-type mice without b8l microglia is more than twice that of controls (Figure 4D), again matching the *Hoxb8* KO phenotype. Similar to *Hoxb8* KO mice, males display more

moderate over-grooming compared to females, apparent in coat-loss penetrance, average amount of coat lost, and average grooming time. Finally, place avoidance typical for mice in an anxiety-like state, cortisol levels, and pupil fight-or-flight reflexes in females but not males (Figures 4E–4G) confirm the same sex-linked pathology observed in *Hoxb8* KO mice. The close match of phenotypes strongly argues for a common disease mechanism in *Hoxb8* KO mutants and mice without b8l microglia that is triggered by the loss of function of this cell type.

## DISCUSSION

Here, we use the mouse as a model system to demonstrate that a microglia subset, derived from *Hoxb8*-expressing precursors, protects from obsessive compulsion and anxiety symptoms. Moreover, we show that female sex hormones worsen the pathology caused by dysfunction in this microglia subset.

### What Is Unique about Hoxb8-Lineage Microglia?

Our ablation strategy efficiently targeted Hoxb8-lineage microglia and caused a pathology without affecting overall microglia counts. Thus, non-targeted microglia must have adaptively filled the Hoxb8-lineage microglia niche but failed to execute Hoxb8-lineage microglia specific functions. The ability of Hoxb8-lineage microglia to suppress over-grooming and anxiety-like behavior in mice suggests a unique molecular machinery in this subtype. In fact, a number of transcripts are more abundant in Hoxb8-lineage than in non-Hoxb8-lineage lineage microglia of adults (De et al., 2018). Differences in gene expression may even be more dramatic during brain development and before behavioral defects manifest. If so, the pathology mediated by malfunctioning Hoxb8-lineage microglia might also be set long before the appearance of behavioral symptoms. Such a scenario is likely for two reasons. First, our data suggest that Hoxb8 is essential for normal Hoxb8-lineage microglia function, even though expression of this transcription factor ceases at around E12 (De et al., 2018). Second, pharmacological ablation of microglia in adult mice, including Hoxb8-lineage microglia, did not result in the obsessive compulsion or anxiety-like behavior reported here (Elmore et al., 2014; Acharya et al., 2016; Rice et al., 2015; Parkhurst et al., 2013). One way to interpret this finding is that Hoxb8-lineage microglia already completed their protective function before they were ablated in adult mice. It would be interesting to see if, for example, Hoxb8-lineage microglia prepare the developing brain circuitry for a balanced response to sex hormones later in life by limiting the number of estrogen and progesterone sensitive synapses (Baudry et al., 2013). In this light, the somewhat milder phenotype in the ablation model compared to mice with germline *Hoxb8* dysfunction might be explained by the small number of remaining functional Hoxb8-lineage microglia that ameliorate the pathology.

### Alternative Perspectives in Microglia Biology

Our finding that the selective loss of Hoxb8-lineage microglia causes pathological behavior is important for two main reasons. First, it illustrates a case in which functions in microglia are distributed over distinct cell lineages. Second, it shows that microglia have the potential to suppress rather than promote the development of obsessive compulsion or anxiety-related

disorders (Stein et al., 2017; Wang et al., 2018; Li et al., 2016; Ma et al., 2015; Piirainen et al., 2017; Ramirez et al., 2017; Li et al., 2014; McKim et al., 2018). A closer look at these two aspects in microglia biology should help to better understand and, consequently, better treat OCD and anxiety.

### Translational Relevance of Our Findings

Over-grooming, anxiety-like behavior, and exaggerated stress responses described here closely resemble symptoms of anxiety disorders in humans. According to the National Institute of Mental Health, almost 20% of all adults in the United States experience at some point an anxiety disorder with a higher prevalence in women (23.4%) than in men (14.3%). Statistics are even more dramatic in adolescents, with 38% of females and 26% of males reporting disabling anxiety. Genetic predisposition appears to be a risk factor for anxiety disorders, yet genetic factors contributing to anxiety susceptibility are difficult to isolate (Morris-Rosendahl, 2002). These difficulties arise from the fact that anxiety occurs sporadically, comprises variable clinical presentations, is heavily influenced by environmental factors, shows comorbidity with other disorders, and is not readily diagnosed. Similarly to the genetic causes, we still have limited understanding of why females are more frequently affected by anxiety than males. A wide range of candidate mechanisms for female anxiety have been proposed, including sex chromosome-dependent gene expression and brain development (Donner and Lowry, 2013). The pathology in our genetically modified mice connects multiple anxiety symptoms and is more severe in females. In *Hoxb8* KO mice, the severity of symptoms in males and females separates at the beginning of sexual maturity. Moreover, the more severe pathology in females is attenuated by treatments that lower female sex-hormone levels and can be simulated in males by supplementing progesterone and β-estradiol. Together, these findings suggest a mechanistic link between genetic changes and being female in the development of anxiety. Another curious finding is that dysfunction of Hoxb8-lineage microglia produces over-grooming in both genders, but marked anxiety-like responses only in females. These observations suggest that OCD- and anxiety-like pathologies are related, but dissociable. This matches the recognized but still unresolved relationship between OCD and anxiety in humans (Stein et al., 2010). Given the enormous impact of anxiety-related disorders to human health, our results further encourage exploration of normal and aberrant Hoxb8-lineage microglia function in the search for improved treatments.

## STAR⋆METHODS

### LEAD CONTACT AND MATERIALS AVAILABILITY

Further information and requests for resources and reagents should be directed to and will be fulfilled by the Lead Contact, Dimitri Tränkner (dtrankner@genetics.utah.edu). All materials are available after completion of the respective material transfer agreements.

### EXPERIMENTAL MODEL AND SUBJECT DETAILS

**Animals—**All experiments described in this study have been performed on mice. Experimental procedures were approved by the Institutional Animal Care and Use Committee at the University of Utah. Mice are housed in groups of 2 to 4 animals under

reversed 12 hour light-dark cycle with *ad libitum* access to water and food in static isolator cages. Unless otherwise stated, experiments were performed with 2–6 months old animals. Sex of animals tested is reported in results and figures. Wild-type mice are C57BL/6J. All other strains were backcrossed to C57BL/6J mice over ≥ 5 generations prior to breeding of experimental mice. Assays were performed on test naive animals, pharmacological treatments were started with drug naive animals.

## METHOD DETAILS

**Generating Hoxb8$^{mut\text{-}IRES\text{-}Cre}$ Mice—***Hoxb8*$^{mut\text{-}IRES\text{-}Cre}$ mice were generated from *Hoxb8*$^{IRES\text{-}Cre}$ using CRISPR/Cas9 mutagenesis (Yang et al., 2013) to replace the wild-type homeodomain DNA-binding site of Hoxb8 (I192-WFQNR198R) with the low DNA-affinity sequence AEFAAAA. In brief, zygotes were injected with 100ng/μL Cas9 mRNA, 50 ng/ μL *Hoxb8* sgRNA, and 100ng/μL single-stranded donor DNA (IDT Technologies) in RNase-free water. RNA was generated and purified using the Life Technologies products mMESSAGE mMACHINE T7 ULTRA kit (Cas9 mRNA), MEGAshortscript T7 kit (*Hoxb8* sgRNA), and MEGAclear kit. The 142 nucleotide Donor DNA included the mutated sequence gccgaattcgccgctgcggc (wild-type: atctggttccagaatcggag) and a novel EcoRI restriction site. *Hoxb8*$^{IRES\text{-}Cre}$ and *Hoxb8*$^{mut\text{-}IRES\text{-}Cre}$ were genotyped using primers gccagacctacagtcgctacca (forward) and cttcttgtcacccttctgcgcatcg (reverse). EcoR1 cleaves the resulting 350bp amplicon of *Hoxb8*$^{mut\text{-}IRES\text{-}Cre}$ into 200bp and 150bp fragments.

**Cell and Tissue Analyses—**Tissue-resident cells were counted in fixed (4% paraformaldehyde in phosphate-buffered saline (PBS)) and stained 100 μm sections. Sections were stained using either anti-RFP (Rockland) or anti-Iba1 (Wako) antibodies in combination with Alexa Fluor 555 (Invitrogen) in 3% bovine serum albumin/0.2% Triton x-100/PBS. Stained and mounted sections were imaged using a Leica TCS SP5 confocal microscope and LAS X software. Maximum intensity projections were manually counted and cell densities calculated using measured slice volumes. Cell counts were verified semi-automatically using ImageJ. For brain gross anatomy inspection, fixed slices were stained with 1:1000 Neurotrace 500/525 green (Life Technologies) in PBS before imaging. White blood cells were counted from ≥.4 μL whole blood samples treated twice with RBC lysis buffer (BioLegend). White blood cells were stained with anti-CD11b-APC (BioLegend), anti-CD45-FITC (BioLegend), and DAPI (Invitrogen) in cell stain buffer (BioLegend). Stained cells were analyzed using a BD FACSCanto flow cytometer and FlowJo software. Relative counts include DAPI-negative, CD45-/tdTomato-positive cells.

**Hormone Measurements—**Urine cortisol, progesterone, and 17β-estradiol were measured using immune enzyme assays and normalized to urine creatinine (all tests Arbor Assays). Test and control samples, about 100 μl per mouse, were collected in parallel over the course of 2–4 h and frozen at −80C for up to one week before assays.

**Urocortin Treatment—**Animals were injected over 5 min with 0.5 μl phosphate-buffered saline (PBS) with or without mouse urocortin II (Sigma-Aldrich, 240 pmol) through pre-implanted cannulas under isoflurane anesthesia. Cannulas (stainless steel, 4mm, 22 Gauge) were capped (C315IS-4/SPC internal 33GA, Plastics One) and implanted ≥ 7 days before

testing 0.5 mm rostral to Bregma at the midline without penetrating the dura mater. Injections were performed using pulled (Model P-87, Sutter) glass micropipettes (Wiretrol II) and a micro-injector (MO-10, Narishige) in a stereotactic apparatus (Model 900, David Kopf Instruments). Injections were placed 2.5 mm below the dura mater. Injected animals recovered for 2–3 h before tests. After testing, animals were injected with 0.5 μl 2% fast green in PBS, euthanized and their brains fixed, sliced, and examined to confirm correct drug placement.

**Trilostane and Hormone Treatment—**Starting at four weeks of age, mice received five daily subcutaneous injections followed by two days without injections for eight weeks (Trilostane; Sigma Millipore) or four weeks (steroid hormones; Sigma Millipore). Doses were (mg/kg weight): 10 Trilostane, 20 17β-Estradiol, 20 progesterone, or 20 17β-Estradiol + 20 progesterone. Drug and hormones were delivered in 20 μl Dimethyl Sulfoxide (dmso; Sigma Millipore). Controls were injected with 20 μl dmso only.

**Ovariectomy—**Ovariectomies are performed on four-week-old females as previously described (Nagy, 2003). In brief, ovaries are pulled through a small skin incision, cut, and removed under general isoflurane anesthesia. Mice undergoing sham ovariectomy only receive the skin incision. Incisions are closed with wound clips. Clips are removed ten days after surgery, again under general anesthesia.

**Behavioral Tests—**Elevated plus maze tests were performed at 100 lux background light using Any-Maze equipment and video-tracking software (Stoelting). Prior to single 5 min tests (Walf and Frye, 2007), mice acclimatized for one hour to the testing room. Grooming times were determined using automatic behavior recognition (Laboras/Metris) in 24-hour tests. Percentage of coat loss was determined from ventral full-body shots and semi-automated custom image analysis software (MATLAB), heat-maps were generated in ImageJ. For pupil tests, animals were implanted with head-posts ≥ 7 days before training sessions. Implanted animals were then trained on 3 consecutive daily sessions (20 min each) to accept the head-fixed configuration. Training and tests were performed inside an isolated test box for controlled ambient light levels of 128 lux and sound levels of 40–45 dB. During the actual test, mice were first accustomed over 5 min to the head-fixed configuration, followed by 20 tone exposures (60 dB, 2 kHz, 5 s duration, 65 s intervals). Pupil images were recorded at 3 Hz under infrared light. For analysis, pupils were identified in each image using Sobel edge finding with MATLAB and pupil area fits verified by visual inspection. Pupil fight-or-flight responses are the average pupil size during the tone minus the average pupil size over the five seconds before the tone (baseline size) and are presented as % baseline size. Only the largest pupil response of each animal contributed to the respective cohort dataset.

## QUANTIFICATION AND STATISTICAL ANALYSIS

We used MATLAB for pupil-size and coat-loss analysis, statistics, and graphs were generated using GraphPad prism. Statistical details are listed in figure legends. Direct comparisons between two data cohorts were performed using non-parametric Mann-Whitney tests. Two factor comparisons testing the effects of sex and genotype, sex and

pharmacological treatment, or cell loss and genotype were performed using standard two-way ANOVA followed by Tukey-Kramer post hoc tests to evaluate the effects of each factor separately. The effects of conditional *Csf1r* deletion, Hoxb8 function, or gender on Hoxb8-lineage microglia depletion were tested using a three-way ANOVA followed by Tukey-Kramer post hoc tests. Significance is equivalent to rejection of the null-hypothesis and given at $p \leq 0.05$. Sample number n refers to the number of mice tested. All statistically evaluated data are presented as bar graphs representing mean and SEM together with individual data points. Time course data are presented as averages across all animals tested within a cohort.

### DATA AND CODE AVAILABILITY

The article includes all datasets generated or analyzed during this study. Software used to generate pupil and coat-loss data are available from the corresponding author on request.

## Supplementary Material

Refer to Web version on PubMed Central for supplementary material.

## ACKNOWLEDGMENTS

We thank Drs. Megan Williams, Adrian Rothenfluh, Yukio Saijoh, and Richard Dorsky for comments on the manuscript. We thank Dr. Monica Vetter for reagents and advice and all members of the Capecchi laboratory, and in particular Kerry Prettyman and Karl Lustig, for general friendly backing of this study. The graphical abstract was made by Dr. Anne Martin, University of Oregon. This study was supported by the National Institutes of Health (NIH) (R01MH093595).

## REFERENCES

Acharya MM, Green KN, Allen BD, Najafi AR, Syage A, Minasyan H, Le MT, Kawashita T, Giedzinski E, Parihar VK, et al. (2016). Elimination of microglia improves cognitive function following cranial irradiation. Sci. Rep 6, 31545. [PubMed: 27516055]

American Psychiatric Association (2013). Diagnostic and Statistical Manual of Mental Disorders: DSM-5. (American Psychiatric Association Publishing).

Anthony TE, Dee N, Bernard A, Lerchner W, Heintz N, and Anderson DJ (2014). Control of stress-induced persistent anxiety by an extra-amygdala septohypothalamic circuit. Cell 156, 522–536. [PubMed: 24485458]

Bandelow B (2008). The medical treatment of obsessive-compulsive disorder and anxiety. CNS Spectr. 13, 37–46. [PubMed: 18849910]

Baudry M, Bi X, and Aguirre C (2013). Progesterone-estrogen interactions in synaptic plasticity and neuroprotection. Neuroscience 239, 280–294. [PubMed: 23142339]

Brioschi S, Peng V, and Colonna M (2019). Fifty Shades of Microglia. Trends Neurosci. 42, 440–443. [PubMed: 31005331]

Chen SK, Tvrdik P, Peden E, Cho S, Wu S, Spangrude G, and Capecchi MR (2010). Hematopoietic origin of pathological grooming in Hoxb8 mutant mice. Cell 141, 775–785. [PubMed: 20510925]

Dai XM, Ryan GR, Hapel AJ, Dominguez MG, Russell RG, Kapp S, Sylvestre V, and Stanley ER (2002). Targeted disruption of the mouse colony-stimulating factor 1 receptor gene results in osteopetrosis, mononu-clear phagocyte deficiency, increased primitive progenitor cell frequencies, and reproductive defects. Blood 99, 111–120. [PubMed: 11756160]

De S, Van Deren D, Peden E, Hockin M, Boulet A, Titen S, and Capecchi MR (2018). Two distinct ontogenies confer heterogeneity to mouse brain microglia. Development 145, dev152306.

Donner NC, and Lowry CA (2013). Sex differences in anxiety and emotional behavior. Pflugers Arch. 465, 601–626. [PubMed: 23588380]

Elmore MR, Najafi AR, Koike MA, Dagher NN, Spangenberg EE, Rice RA, Kitazawa M, Matusow B, Nguyen H, West BL, and Green KN (2014). Colony-stimulating factor 1 receptor signaling is necessary for microglia viability, unmasking a microglia progenitor cell in the adult brain. Neuron 82, 380–397. [PubMed: 24742461]

Erblich B, Zhu L, Etgen AM, Dobrenis K, and Pollard JW (2011). Absence of colony stimulation factor-1 receptor results in loss of microglia, disrupted brain development and olfactory deficits. PLoS ONE 6, e26317. [PubMed: 22046273]

Gellhorn E (1957). Autonomic Imbalance and the Hypothalamus: Implications for Physiology, Medicine, Psychology, and Neuropsychiatry (University of Minnesota Press).

Ginhoux F, and Guilliams M (2016). Tissue-Resident Macrophage Ontogeny and Homeostasis. Immunity 44, 439–449. [PubMed: 26982352]

Hammond TR, Dufort C, Dissing-Olesen L, Giera S, Young A, Wysoker A, Walker AJ, Gergits F, Segel M, Nemesh J, et al. (2019). Single-Cell RNA Sequencing of Microglia throughout the Mouse Lifespan and in the Injured Brain Reveals Complex Cell-State Changes. Immunity 50, 253–271. [PubMed: 30471926]

Han J, Harris RA, and Zhang XM (2017). An updated assessment of microglia depletion: current concepts and future directions. Mol. Brain 10, 25. [PubMed: 28629387]

Henry B, Vale W, and Markou A (2006). The effect of lateral septum corticotropin-releasing factor receptor 2 activation on anxiety is modulated by stress. J. Neurosci 26, 9142–9152. [PubMed: 16957071]

Jimenez JC, Su K, Goldberg AR, Luna VM, Biane JS, Ordek G, Zhou P, Ong SK, Wright MA, Zweifel L, et al. (2018). Anxiety Cells in a Hippocampal-Hypothalamic Circuit. Neuron 97, 670–683. [PubMed: 29397273]

Joe EH, Choi DJ, An J, Eun JH, Jou I, and Park S (2018). Astrocytes, Microglia, and Parkinson's Disease. Exp. Neurobiol 27, 77–87. [PubMed: 29731673]

Korff S, and Harvey BH (2006). Animal models of obsessive-compulsive disorder: rationale to understanding psychobiology and pharmacology. Psychiatr. Clin. North Am 29, 371–390. [PubMed: 16650714]

Krukowski K, Feng X, Paladini MS, Chou A, Sacramento K, Grue K, Riparip LK, Jones T, Campbell-Beachler M, Nelson G, and Rosi S (2018). Temporary microglia-depletion after cosmic radiation modifies phagocytic activity and prevents cognitive deficits. Sci. Rep 8, 7857. [PubMed: 29777152]

Li Q, and Barres BA (2018). Microglia and macrophages in brain homeostasis and disease. Nat. Rev. Immunol 18, 225–242. [PubMed: 29151590]

Li J, Chen K, Zhu L, and Pollard JW (2006). Conditional deletion of the colony stimulating factor-1 receptor (c-fms proto-oncogene) in mice. Genesis 44, 328–335. [PubMed: 16823860]

Li Z, Ma L, Kulesskaya N, Vôikar V, and Tian L (2014). Microglia are polarized to M1 type in high-anxiety inbred mice in response to lipopolysaccharide challenge. Brain Behav. Immun 38, 237–248. [PubMed: 24561490]

Li Z, Wei H, Piirainen S, Chen Z, Kalso E, Pertovaara A, and Tian L (2016). Spinal versus brain microglial and macrophage activation traits determine the differential neuroinflammatory responses and analgesic effect of minocycline in chronic neuropathic pain. Brain Behav. Immun 58, 107–117. [PubMed: 27262531]

Lucin KM, and Wyss-Coray T (2009). Immune activation in brain aging and neurodegeneration: too much or too little? Neuron 64, 110–122. [PubMed: 19840553]

Ma L, Piirainen S, Kulesskaya N, Rauvala H, and Tian L (2015). Association of brain immune genes with social behavior of inbred mouse strains. J. Neuroinflammation 12, 75. [PubMed: 25895500]

Madisen L, Zwingman TA, Sunkin SM, Oh SW, Zariwala HA, Gu H, Ng LL, Palmiter RD, Hawrylycz MJ, Jones AR, et al. (2010). A robust and high-throughput Cre reporting and characterization system for the whole mouse brain. Nat. Neurosci 13, 133–140. [PubMed: 20023653]

McKim DB, Weber MD, Niraula A, Sawicki CM, Liu X, Jarrett BL, Ramirez-Chan K, Wang Y, Roeth RM, Sucaldito AD, et al. (2018). Microglial recruitment of IL-1β-producing monocytes to brain endothelium causes stress-induced anxiety. Mol. Psychiatry 23, 1421–1431. [PubMed: 28373688]

Morris-Rosendahl DJ (2002). Are there anxious genes? Dialogues Clin. Neurosci 4, 251–260. [PubMed: 22033820]

Nagarajan N, Jones BW, West PJ, Marc RE, and Capecchi MR (2018). Corticostriatal circuit defects in Hoxb8 mutant mice. Mol. Psychiatry 23, 1868–1877. [PubMed: 28948967]

Nagy A (2003). Manipulating the Mouse Embryo: A Laboratory Manual (Cold Spring Harbor Laboratory Press).

Nakayama H, Abe M, Morimoto C, Iida T, Okabe S, Sakimura K, and Hashimoto K (2018). Microglia permit climbing fiber elimination by promoting GABAergic inhibition in the developing cerebellum. Nat. Commun 9, 2830. [PubMed: 30026565]

Parkhurst CN, Yang G, Ninan I, Savas JN, Yates JR 3rd, Lafaille JJ, Hempstead BL, Littman DR, and Gan WB (2013). Microglia promote learning-dependent synapse formation through brain-derived neurotrophic factor. Cell 155, 1596–1609. [PubMed: 24360280]

Patriquin MA, and Mathew SJ (2017). The Neurobiological Mechanisms of Generalized Anxiety Disorder and Chronic Stress. Chronic Stress (Thousand Oaks) 1 10.1177/2470547017703993.

Piirainen S, Youssef A, Song C, Kalueff AV, Landreth GE, Malm T, and Tian L (2017). Psychosocial stress on neuroinflammation and cognitive dysfunctions in Alzheimer's disease: the emerging role for microglia? Neurosci. Biobehav. Rev 77, 148–164. [PubMed: 28185874]

Pineda MH, and Dooley MP (2003). McDonald's Veterinary Endocrinology and Reproduction (Iowa State Press).

Potts GO, Creange JE, Hardomg HR, and Schane HP (1978). Trilostane, an orally active inhibitor of steroid biosynthesis. Steroids 32, 257–267. [PubMed: 715820]

Ramirez K, Fornaguera-Trías J, and Sheridan JF (2017). Stress-Induced Microglia Activation and Monocyte Trafficking to the Brain Underlie the Development of Anxiety and Depression. Curr. Top. Behav. Neurosci 31, 155–172. [PubMed: 27352390]

Rice RA, Spangenberg EE, Yamate-Morgan H, Lee RJ, Arora RPS, Hernandez MX, Tenner AJ, West BL, and Green KN (2015). Elimination of Microglia Improves Functional Outcomes Following Extensive Neuronal Loss in the Hippocampus. J. Neurosci 35, 9977–9989. [PubMed: 26156998]

Schafer DP, Lehrman EK, Kautzman AG, Koyama R, Mardinly AR, Yamasaki R, Ransohoff RM, Greenberg ME, Barres BA, and Stevens B (2012). Microglia sculpt postnatal neural circuits in an activity and complement-dependent manner. Neuron 74, 691–705. [PubMed: 22632727]

Schneider CA, Rasband WS, and Eliceiri KW (2012). NIH Image to ImageJ: 25 years of image analysis. Nat. Methods 9, 671–675. [PubMed: 22930834]

Stein DJ, Fineberg NA, Bienvenu OJ, Denys D, Lochner C, Nestadt G, Leckman JF, Rauch SL, and Phillips KA (2010). Should OCD be classified as an anxiety disorder in DSM-V? Depress. Anxiety 27, 495–506. [PubMed: 20533366]

Stein DJ, Vasconcelos MF, Albrechet-Souza L, Ceresér KMM, and de Almeida RMM (2017). Microglial Over-Activation by Social Defeat Stress Contributes to Anxiety- and Depressive-Like Behaviors. Front. Behav. Neurosci 11, 207. [PubMed: 29114211]

Tejera D, and Heneka MT (2016). Microglia in Alzheimer's disease: the good, the bad and the ugly. Curr. Alzheimer Res 13, 370–380. [PubMed: 26567746]

Walf AA, and Frye CA (2007). The use of the elevated plus maze as an assay of anxiety-related behavior in rodents. Nat. Protoc 2, 322–328. [PubMed: 17406592]

Wang YL, Han QQ, Gong WQ, Pan DH, Wang LZ, Hu W, Yang M, Li B, Yu J, and Liu Q (2018). Microglial activation mediates chronic mild stress-induced depressive- and anxiety-like behavior in adult rats. J. Neuroinflammation 15, 21. [PubMed: 29343269]

Yang H, Wang H, Shivalila CS, Cheng AW, Shi L, and Jaenisch R (2013). One-step generation of mice carrying reporter and conditional alleles by CRISPR/Cas-mediated genome engineering. Cell 154, 1370–1379. [PubMed: 23992847]

## Highlights

- A microglia sublineage derived from Hoxb8-expressing precursors serves unique functions
- Dysfunction of Hoxb8-lineage microglia causes anxiety symptoms and obsessive compulsion
- Female sex hormones worsen the pathology caused by Hoxb8-lineage microglia dysfunction

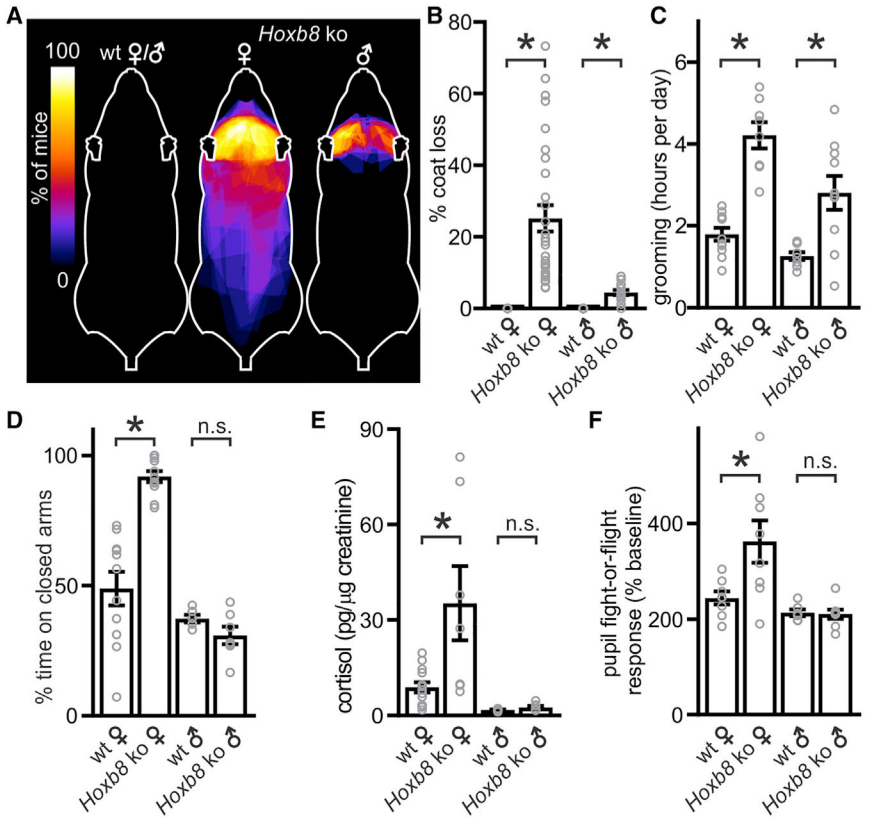


**Figure 1. Hoxb8 Knockout Mice Display Sex-Linked Over-Grooming and Anxiety-like Behavior**

(A) Heatmaps illustrating coat loss penetrance in adult (≥3 month) *Hoxb8* knockout (KO) females and males, wild-type (WT) controls do not show coat loss.

(B) Direct comparisons of coat loss in females (WT: n = 11, *Hoxb8* KO: n = 29; $p < 0.0001$) and males (WT: n = 16, *Hoxb8* KO: n = 13; $p < 0.0001$). Two-way ANOVA and post hoc tests show significant effects of genotype ($p < 0.0001$) and sex ($p = 0.003$).

(C) Direct comparisons of grooming in females (WT: n = 11, *Hoxb8* KO: n = 8; $p < 0.0001$) and males (WT: n = 9, *Hoxb8* KO: n = 10; $p = 0.008$). Two-way ANOVA and post hoc tests show significant effects of genotype ($p < 0.0001$) and sex ($p = 0.001$).

(D) Percent time spent on the closed arms of an elevated plus maze show a marked difference between WT and *Hoxb8* KO females (WT: n = 11, *Hoxb8* KO: n = 11; $p < 0.0001$) but not males (WT: n = 6, *Hoxb8* KO: n = 7; $p = 0.18$). Two-way ANOVA and post hoc tests show significant effects of genotype ($p = 0.0005$) and sex ($p < 0.0001$).

(E) Similarly, cortisol levels are different between WT and *Hoxb8* KO females (WT: n = 13, *Hoxb8* KO: n = 9; $p = 0.007$) but not males (WT: n = 7, *Hoxb8* KO: n = 7; $p = 0.21$). Two-way ANOVA and post hoc tests show significant effects of genotype ($p = 0.025$) and sex ($p = 0.001$).

(F) Pupil fight-or-flight responses are also different between WT and *Hoxb8* KO females (WT: n = 8, *Hoxb8* KO: n = 8; $p = 0.03$) but not males (WT: n = 6, *Hoxb8* KO: n = 8; $p = 0.95$). Two-way ANOVA and post hoc tests show significant effects of genotype ($p = 0.04$) and sex ($p = 0.002$).

Bar graphs show mean and SEM; gray circles are individual data points. Direct comparison: Mann-Whiney test; asterisks indicate significant differences; n.s. indicates non-significant differences. Post hoc test: Tukey-Kramer.

See also Figure S1 and Table S1.

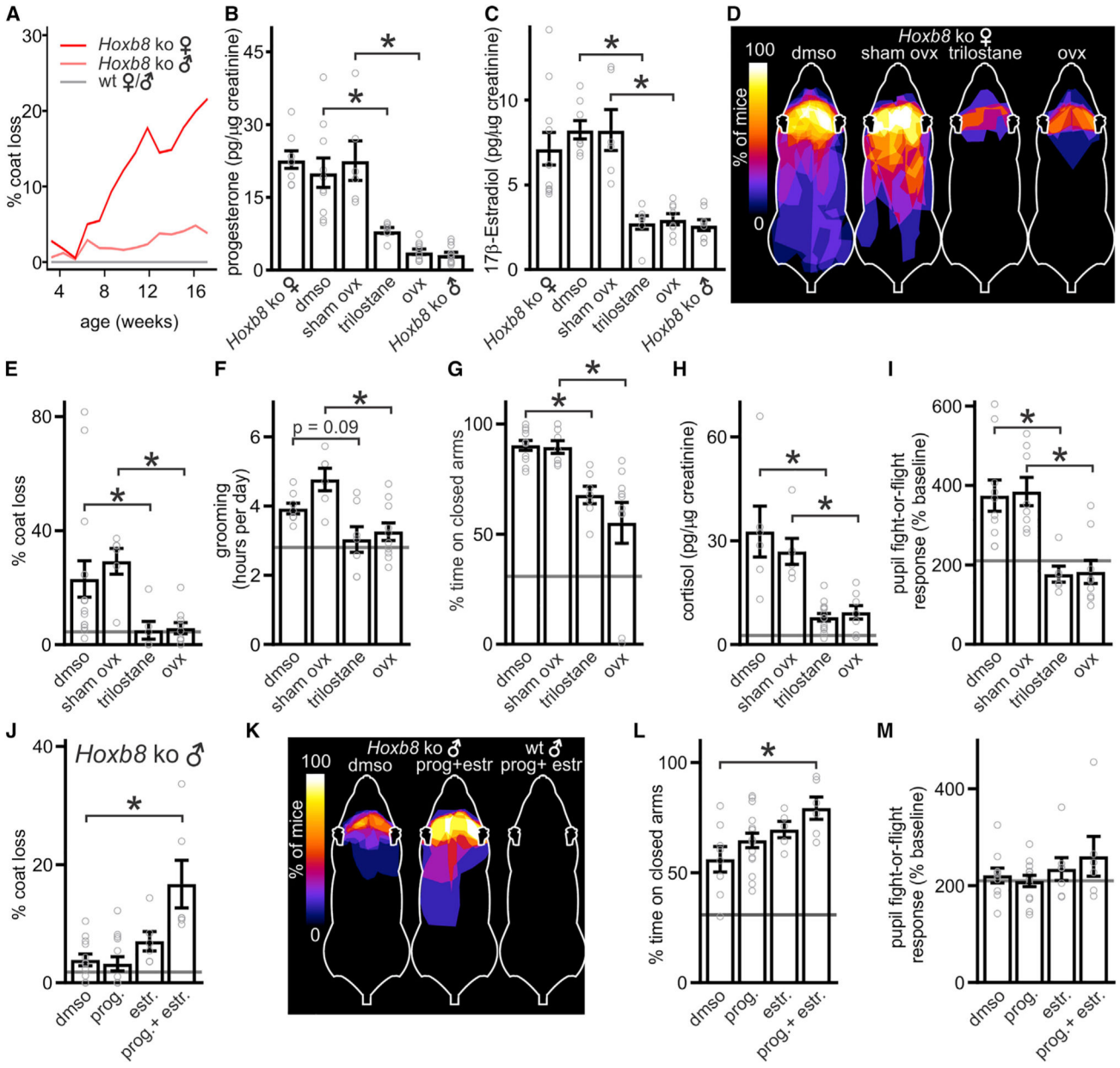


**Figure 2. Female Sex Hormones Set the Severity of the Hoxb8 KO Pathology**

(A) Differences in coat loss severity between *Hoxb8* KO males and females become apparent at the beginning of sexual maturity (~6 weeks). Shown are averages measured weekly for at least four mice per age, sex, and genotype.

(B and C) Trilostane treatment (B) or ovariectomy (ovx) (C) lower urine progesterone and 17β-estradiol to levels closer to those found in males (progesterone: n = 13, 17β-estradiol: n = 8). Progesterone levels in ovx (n = 11) or trilostane-treated (n = 7) *Hoxb8* KO females are different from those in sham ovx (n = 6) or DMSO-treated (n = 10) *Hoxb8* KO females, respectively ($p \leq 0.0002$). Similarly, 17β-estradiol levels in ovx (n = 8) or trilostane-treated (n = 7) *Hoxb8* KO females are different from those in sham ovx (n = 6) or DMSO-treated (n = 8) *Hoxb8* KO females ($p \leq 0.0007$).

(D) Heatmaps illustrating coat loss penetrance in 3-month-old DMSO-treated (n = 15), sham ovx (n = 6), trilostane-treated (n = 6), or ovx (n = 10) *Hoxb8* KO females. Daily treatments started/surgeries were performed 2 months before coat loss measurements.
(E) Coat loss of ovx or trilostane-treated *Hoxb8* KO females is significantly less than in the respective controls ($p \geq 0.014$).
(F) Less severe coat loss is reflected in reduced average grooming time of ovx (n = 10) or trilostane-treated (n = 6) *Hoxb8* KO females compared to sham ovx (n = 6; $p = 0.005$) or DMSO-treated (n = 8; $p = 0.09$) controls, respectively.
(G–I) Ovx and trilostane treatment diminish anxiety-like place avoidance in the elevated plus maze (G), as well as the cortisol (H) and pupil fight-or-flight (I) stress responses, compared to the respective controls ($n \geq 6$ mice each; $p \leq 0.0025$).
(J) Percent coat loss of 8-week-old *Hoxb8* KO males after 4 weeks of daily injections with vehicle DMSO (n = 12), progesterone (n = 13), 17β-estradiol (n = 6), or both combined (n = 6). The combination of progesterone and 17β-estradiol produces a significant increase in coat loss compared to vehicle alone ($p = 0.0002$).
(K) Heatmaps illustrating coat-loss penetrance in DMSO (left) versus progesterone + 17β-estradiol-treated *Hoxb8* KO males (middle). Progesterone + 17β-estradiol treatment does not produce coat loss in WT males (right).
(L and M) Elevated plus maze place avoidance (L) and pupil fight-or-flight stress responses (M) in *Hoxb8* KO males treated with female sex hormones or vehicle alone ($n \geq 5$ mice each). Gray lines mark averaged results for untreated *Hoxb8* KO males.
Bar graphs show mean and SEM; gray circles are individual data points. Direct comparison: Mann-Whiney test; asterisks indicate significant differences. See also Figure S2 and Table S1.

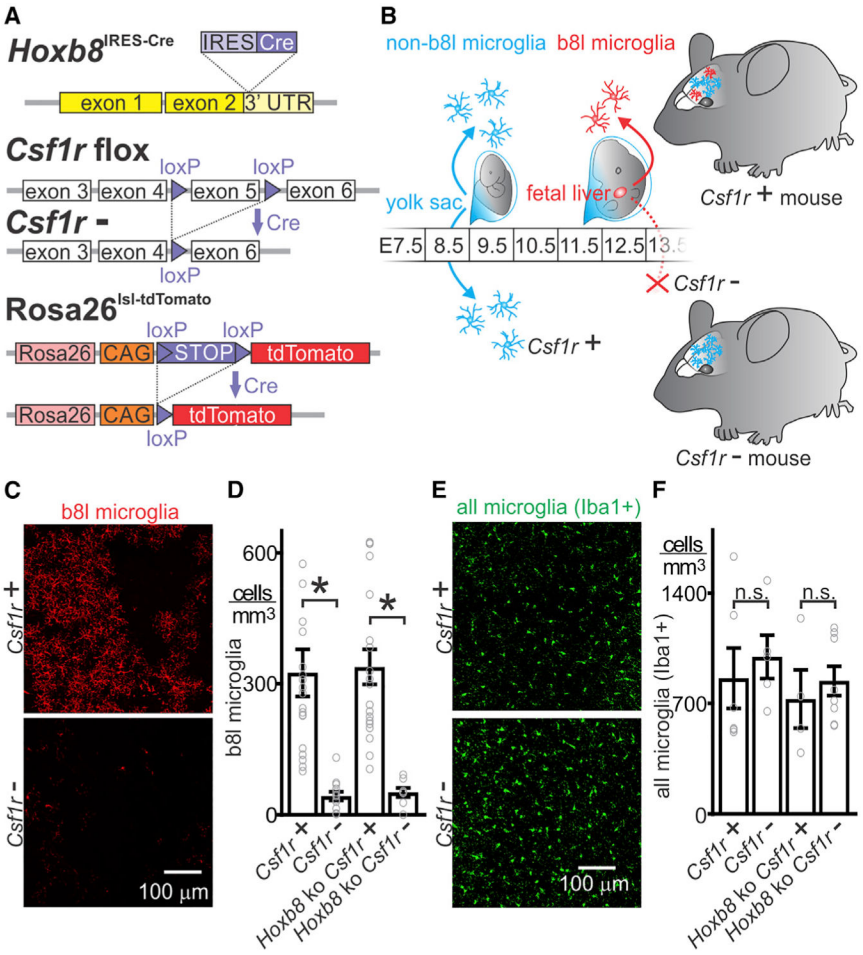


**Figure 3. Selective Ablation of Hoxb8-Line-age (b8l) Microglia**

(A) Schematic of engineered alleles for Cre expression under the *Hoxb8*-promotor (top), and Cre-dependent disruption of the colony-stimulating factor 1 receptor (*Csf1r*) gene (middle) and tdTomato expression (bottom).

(B) Schematic of microglia ontogeny in mice with normal (*Csf1r*$^{+}$) and disrupted Csf1r (*Csf1r*$^{-}$) function in Hoxb8 cells.

(C) Confocal images of coronal 100 µm brain section at bregma +1.10 mm of a *Csf1r*$^{+}$ mouse showing tdTomato-positive b8l microglia (upper). These cells are depleted in *Csf1r*$^{-}$ mice (lower).

(D) B8l microglia counts drop from 312 ± 53 cells/ mm$^3$ in *Csf1r*$^{+}$ mice (n = 19; 9 females, 10 males) to 43 ± 10 cells/mm$^3$ in *Csf1r*$^{-}$ mice (n = 13; 9 females, 4 males; $p < 0.0001$). The loss of b8l microglia on *Hoxb8* KO background is similar and drops from 339 ± 40 cells/mm$^3$ in *Hoxb8* KO *Csf1r*$^{+}$ (n = 19; 6 females, 13 males) to 51 ± 10 cells/mm$^3$ in *Hoxb8* KO *Csf1r*$^{-}$ mice (n = 8; 5 females, 3 males; $p < 0.0001$). Two-way ANOVA and post hoc tests show that b8l microglia counts depend on Csf1r ($p < 0.0001$), but not on Hoxb8 ($p = 0.81$) function. Three-way ANOVA and post hoc tests show no effect of gender on the ablation efficiency ($p = 0.78$). (E) Confocal images showing all microglia (stained for Iba1) in adjacent 100-µm sections (bregma + 0.14 mm) from a *Csf1r*$^{+}$ (upper) and a *Csf1r*$^{-}$ (lower) mouse.

(F) Total microglia counts are similar in *Csf1r*$^{+}$ and *Csf1r*$^{-}$ mice in both *Hoxb8* WT and KO background ($p \geq .43$). *Csf1r*$^{+}$: n = 6; 3 females, 3 males. *Csf1r*$^{-}$: n = 5; 3 females, 2 males. *Hoxb8* KO *Csf1r*$^{+}$: n = 4; 2 females, 2 males. *Hoxb8* KO *Csf1r*$^{-}$: n = 8; 4 females, 4 males. Two-way ANOVA and posthoc tests show that the total microglia count does not depend on Csf1r ($p = 0.42$) or Hoxb8 ($p = 0.37$) function.

Bar graphs show mean and SEM; gray circles are individual data points. Asterisks indicate statistically significant differences; n.s. indicates non-significant differences (Mann-Whitney test).

See also Figure S3 and Table S1.

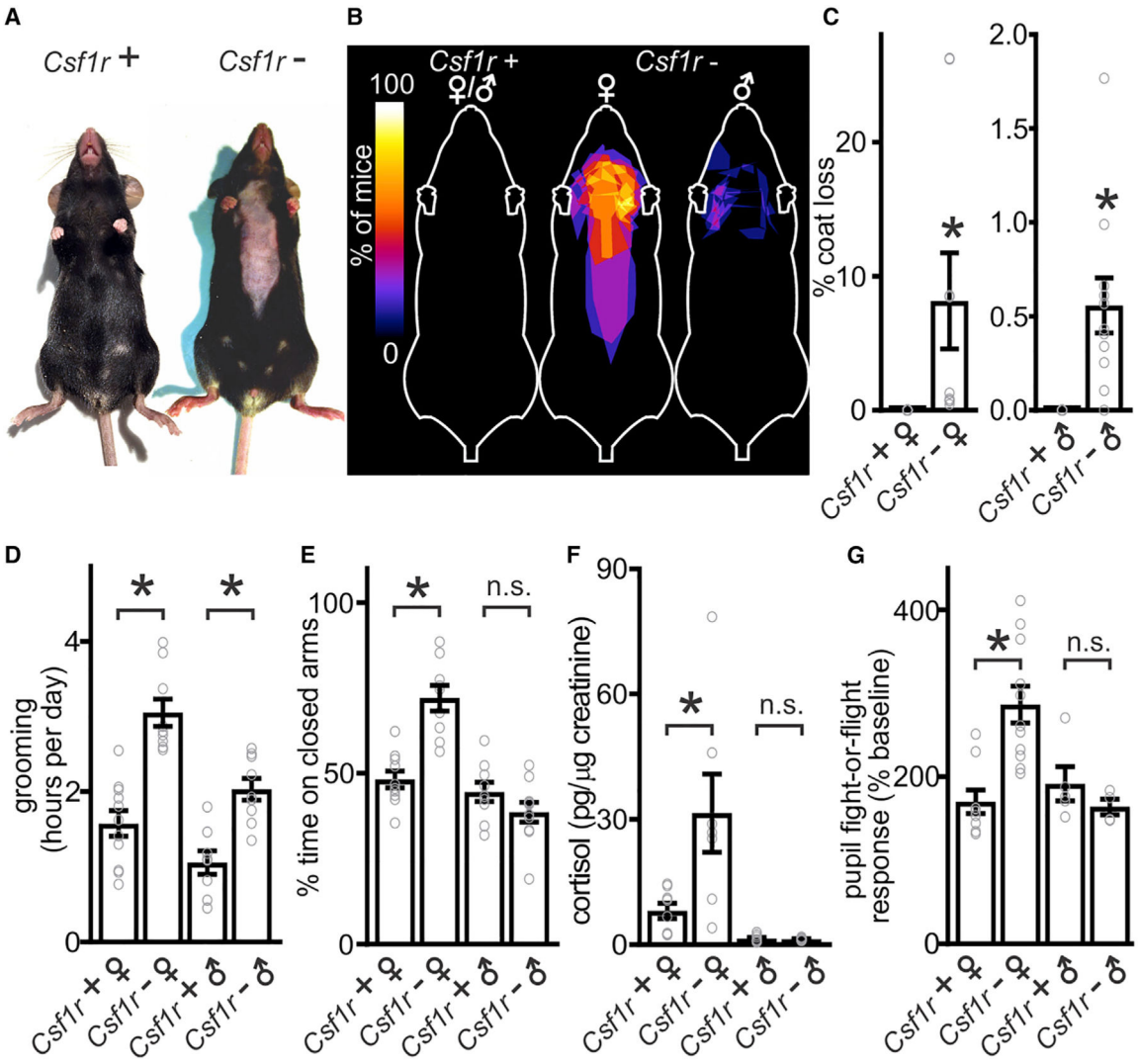


**Figure 4. The Pathology in Mice without b8l Microglia Phenocopies that of Hoxb8 KO Mice**

(A) *Csf1r*$^{-}$ mice display ventral coat loss.

(B) Heatmaps illustrating coat-loss penetrance in adult *Csf1r*$^{-}$ females and males, *Csf1r*$^{+}$ controls do not show coat loss.

(C) Coat loss is statistically significant in both female (left; *Csf1r*$^{+}$: n = 11, *Csf1r*$^{-}$: n = 9; $p < 0.0001$) and male (right; *Csf1r*$^{+}$: n = 8, *Csf1r*$^{-}$: n = 11; $p = 0.0002$) *Csf1r*$^{-}$ mice. Similar to the phenotype in mice with *Hoxb8* loss, two-way ANOVA and post hoc tests show significant effects of b8l microglia loss ($p = 0.01$) and sex ($p = 0.03$).

(D) Direct comparisons of grooming in females (*Csf1r*$^{+}$: n = 11, *Csf1r*$^{-}$: n = 9; $p < 0.0001$) and males (*Csf1r*$^{+}$: n = 8, *Csf1r*$^{-}$: n = 9; $p < 0.001$). Two-way ANOVA and post hoc tests show significant effects of b8l microglia loss ($p < 0.0001$) and sex ($p < 0.0001$).

(E) Percent time spent on the closed arms of an elevated plus maze show a marked difference between *Csf1r*$^{+}$ and *Csf1r*$^{-}$ females (*Csf1r*$^{+}$: n = 10, *Csf1r*$^{-}$: n = 9; $p < 0.0001$) but not males (*Csf1r*$^{+}$: n = 9, *Csf1r*$^{-}$: n = 10; $p = 0.18$). Two-way ANOVA and post hoc tests show significant effects of b8l microglia loss ($p = 0.005$) and sex ($p < 0.0001$).

(F) Similarly, cortisol levels are different between *Csf1r*$^{+}$ and *Csf1r*$^{-}$ females (*Csf1r*$^{+}$: n = 8, *Csf1r*$^{-}$: n = 7; p = 0.02) but not males (*Csf1r*$^{+}$: n = 8, *Csf1r*$^{-}$: n = 8; p = 0.21). Two-way ANOVA and post hoc tests show significant effects of b8l microglia (p = 0.01) and sex (p = 0.0002).

(G) Pupil fight-or-flight responses are also different between *Csf1r*$^{+}$ and *Csf1r*$^{-}$ females (*Csf1r*$^{+}$: n = 9, *Csf1r*$^{-}$: n = 10; p = 0.0004) but not males (*Csf1r*$^{+}$: n = 5, *Csf1r*$^{-}$: n = 4; p = 0.29). Two-way ANOVA and post hoc tests show significant effects of b8l microglia loss (p = 0.03) and sex (p = 0.02).

Bar graphs show mean and SEM; gray circles are individual data points. Direct comparison: Mann-Whitney test; asterisks indicate significant differences; n.s. indicates non-significant differences. Post hoc test: Tukey-Kramer.

See also Figure S4 and Table S1.

## KEY RESOURCES TABLE

| REAGENT or RESOURCE | SOURCE | IDENTIFIER |
|---|---|---|
| Antibodies | | |
| anti-RFP | Rockland | Cat#600-401-379; RRID:AB_2209751 |
| anti-lba1 | Wako | Cat#019–19741; RRID:AB_839504 |
| Alexa Fluor 555 | Invitrogen | Cat#A31572; RRID:AB_162543 |
| anti CD11b-APC | BioLegend | Cat#101212; RRID: AB_312795 |
| anti CD45-FITC | BioLegend | Cat#103108; RRID: AB_312973 |
| Chemicals, Peptides, and Recombinant Proteins | | |
| Urocortin II | Millipore-Sigma | Cat# U9507 |
| Trilostane | Millipore-Sigma | Cat#SML0141 |
| Estrogen | Millipore-Sigma | Cat#PHR1353 |
| Progesterone | Millipore-Sigma | Cat#P3972 |
| Critical Commercial Assays | | |
| Cortisol ELISA Kit | Arbor Assays | Cat#K003 |
| Estradiol ELISA Kit | Arbor Assays | Cat#K030 |
| Progesterone ELISA Kit | Arbor Assays | Cat#K025 |
| Creatinine Urinary Detection Kit | Arbor Assays | Cat#K002 |
| Deposited Data | | |
| raw and analyzed data | This paper | N/A |
| Experimental Models: Organisms/Strains | | |
| *Hoxb8* ko | Mario Capecchi | RRID 4818890 |
| *Hoxb8*$^{IRES-Cre}$ | Mario Capecchi | RRID 4837097 |
| *Hoxb8*$^{mut-IRES-Cre}$ | This paper | N/A |
| *Csf1r*$^{flox}$ | The Jackson Laboratory | Stock# 021212; RRID 3653677 |
| Rosa26$^{lsl-tdTomato}$ | The Jackson Laboratory | Stock# 007914; RRID 4436847 |
| Oligonucleotides | | |
| *Hoxb8*$^{mut-IRES-Cre}$ genotyping primer: gccagacctacagtcgctacca (forward) | This paper | N/A |
| Hoxb8$^{mut-IRES-Cre}$ genotyping primer: cttcttgtcacccttctgcgcatcg (reverse) | This paper | N/A |
| Software and Algorithms | | |
| MATLAB and Image Acquisition/Image Processing Toolboxes Release 2015a | The MathWorks, Inc. | https://www.mathworks.com/products/get-matlab.html?s_tid=gn_getml |
| Leica Application Suite X | Leica Microsystems | https://www.leica-microsystems.com/products/microscope-software/p/leica-las-x-ls/ |
| ImageJ | Schneider et al., 2012 | https://imagej.nih.gov/ij/ |
| FlowJo | FlowJo, LLC | https://www.flowjo.com/solutions/flowjo/downloads |
| GraphPad Prism version 8.0.0 | GraphPad Software | https://www.graphpad.com |